

Structure-properties relationships for densely cross-linked epoxide-amine systems based on epoxide or amine mixtures

Part 3 *Elastic Properties*

E. MOREL*, V. BELLENGER[‡], M. BOCQUET[‡], J. VERDU[‡]

* IRCHA BP 1, 91710 vert le petit, France and [‡] ENSAM, 151 B^d de l'Hôpital, 75640 Paris, CEDEX 13, France

Tensile (293 K), dynamic (210 to 570 K, 0.3 Hz), and ultrasonic (293 K, 5 MHz) moduli were determined for various epoxy networks based on epoxide or amine mixtures. Crosslink density and glass transition temperature have an insignificant influence on the elastic properties in glassy state which are mainly controlled by the cohesive energy. Various methods of modulus prediction from structure were compared and discussed. They have generally a low predictive value because many types of hydrogen bonds, having very different contributions to the cohesion, coexist in epoxies. An interesting correlation was found between ultrasonic moduli and water absorption. The incidence of beta relaxations on the elastic properties determined at room temperature and low strain rate was examined. It appeared that an internal plasticizer as aniline increases the glassy state rigidity by suppression of the beta relaxation without noticeable change of packing density. A possible generalization of this latter result was discussed.

1. Introduction

Despite the relatively large amount of data available in the literature on elastic properties of amine cross-linked epoxies in glassy state, it seems difficult to make a coherent synthesis because the trends of structure-modulus relationships seem to be contradictory from one sample family to another. It was found for instance that in some cases, the tensile or bulk modulus decreases when the crosslink density (and the glass transition temperature T_g) increases, [1-3]. In other cases however, the rigidity was found practically independent of the crosslink density [4], whereas it increases with the conversion of the amine-epoxide reaction for a given stoichiometric system [5].

For the first category of studies, the density varied in the same way as the modulus, which led the authors to interpret their results in terms of packing density decrease or free volume increase due to steric restrictions in densely crosslinked glasses. In many cases, however, the density increases with the crosslink density [4, 6]. Furthermore the density variations cannot be systematically assimilated to variations of the packing density except when the chemical composition is constant which was not the case.

It therefore seems interesting to determine the specific features of the systems under study, probably by investigating a large number of systems including various distinct structural series. Single data obtained at a given temperature in a given time scale are generally insufficient to establish structure-properties relationships, owing to the complications due to viscoelastic effects. From this point of view, measurements made at high frequency, (sound or ultrasound propagation

rate), are probably easier to correlate with molecular structure than more classical data obtained, for instance from tensile or compression test.

The aim of this work is to compare the elastic moduli of 14 aromatic-rich epoxide-amine networks of moderate or high crosslink density ($n \geq 2 \text{ mol kg}^{-1}$), and to try to correlate it with structure. In all cases, tensile static, flexural dynamic and ultrasonic measurements were made.

2. Experimental procedure

2.1. Materials

The systems were based on epoxide or amine mixtures. Some of their physical properties: glass transition temperature, density, water absorption, were described in the preceding parts of this article and are recalled in Table I. Three families were studied: A, mixture of diglycidyl ether of bisphenol A (DGEBA) with triglycidyl *p*-amino phenol (TGAP) crosslinked by diamino diphenyl methane (DDM); B, mixture of DGEBA with TGAP crosslinked by the tetraethyl derivative of DDM (DDMe); C, TGAP crosslinked a mixture of DDM and aniline. The same bars as in preceding parts (3 mm thickness), were used for tensile and dynamic flexural tests. For ultrasonic (US) measurements, (25 × 25 × 7.5 mm) samples molded in the same conditions as tensile bars, were used. It was not possible to obtain C.100 (TGAP-aniline) samples of such thickness owing to the high exothermicity of the cure reactions.

2.2. Measurements

Tensile tests were made with an INSTRON machine

TABLE I Composition and physical properties of the systems under study

Code	DGEBA % (a)	TGAP % (a)	DDM % (b)	Aniline % (b)	DDM _e % (b)	T _g (K)	ρ	ρ* (c)
A0	100	0	100	0	0	443	1.200	0.678
A25	75	25	100	0	0	466	1.217	0.684
A50	50	50	100	0	0	472	1.238	0.693
A80	20	80	100	0	0	486	1.257	0.700
A100	0	100	100	0	0	499	1.269	0.703
C25	0	100	75	25	0	470	1.263	0.702
C50	0	100	50	50	0	440	1.263	0.703
C75	0	100	25	75	0	408	1.259	0.702
C100	0	100	0	100	0	391	1.255	0.700
B0	100	0	0	0	100	417	1.152	0.676
B25	75	25	0	0	100	439	1.154	0.678
B50	50	50	0	0	100	456	1.162	0.683
B75	25	75	0	0	100	464	1.172	0.690
B100	0	100	0	0	100	471	1.175	0.692

(a) weight percent in the epoxide mixture.

(b) weight percent in the amine mixture.

(c) see the definition and mode of calculation in appendix.

at 20°C, 0.00016 sec⁻¹ strain rate unless specified. Measurements were made on a dozen samples for each system. The data acquisition system allows the automatic determination of the tangent modulus. Only the average value will be reported, the standard deviation was typically ≈ 5%. The dynamic flexural measurements were made with a DMTA (Polymer Laboratories, Epirial Way, Loughborough, UK) apparatus in the 213 to 753 K range at 0.3 Hz frequency and 3 K min⁻¹ scanning rate. The free length/thickness ratio was about 5, e.g. far from the geometric requirements needed for rigorous modulus measurements ($L/th \geq 40$). The results can however be used in a comparative way.

Ultrasonic measurements were made at 5 MHz using pulse methods [7] schematized in Fig. 1. The precision and reproducibility essentially depend on how planar and how parallel are the sample surfaces. They were less than 2% in the cases under study. The moduli were calculated using the following relations [8]

$$v_L^2 = \frac{B}{\rho} \frac{3(1-\nu)}{1+\nu} \quad (1)$$

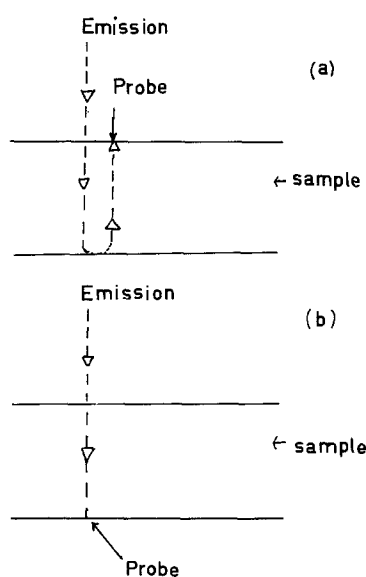


Figure 1 Schematic representation of the measurement method for ultrasonic longitudinal (a) and transversal (b) waves. Velocities are deduced from the time elapsed between emission and reception of a pulse.

$$v_T^2 = \frac{G}{\rho} \quad (2)$$

$$E = 3B(1 - 2\nu) = 2G(1 + \nu) \quad (3)$$

where v_L and v_T are respectively the longitudinal and transversal wave propagation rates, E , B and G are respectively the Young's, bulk and shear moduli, ρ is the density and ν the Poisson's ratio.

3. Results

3.1. Tensile moduli

For two different samples: B100 and C100, the modulus was measured at various strain rates between 1.6×10^{-5} and 1.6×10^{-3} sec⁻¹. The results presented in Fig. 2 show that at 20°C the modulus varies only slightly with the strain rate (≈ 5% per decade). The results obtained with a strain rate of 1.6×10^{-4} sec⁻¹ and some important characteristics of the samples under study are given in Table II. The modulus E_T was plotted against the crosslink density n in Fig. 3 and the hydroxyl concentration [OH] in Fig. 4. Plots of E_T against T_g or packing density ρ^* , would display the same trends as in Fig. 3. Plots of E_T against

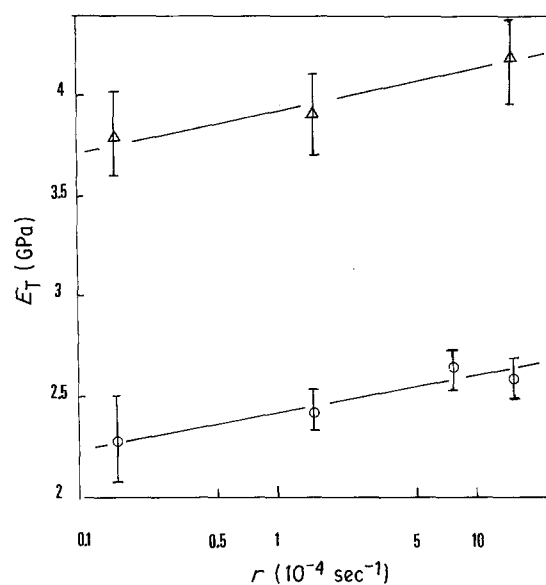


Figure 2 Influence of the strain rate on the tensile modulus for samples B100 (O) and C100 (Δ).

TABLE II Crosslink density n , concentration of aromatic nuclei ϕ and hydroxyl groups [OH], tensile modulus E_T and dynamic modulus E_D' , both measured at 293 K

Code	$n(\text{M Kg}^{-1})$	$\phi(\text{M Kg}^{-1})$	[OH](M Kg^{-1})	E_T (GPa)	E_D (GPa)
A0	2.28	6.83	4.56	2.35	1.32
A25	3.30	6.56	5.26	2.62	1.48
A50	4.23	6.31	5.91	2.70	1.62
A80	5.25	6.04	6.62	3.22	1.29
A100	5.88	5.88	7.05	3.25	1.68
C25	4.98	5.91	7.09	3.53	1.60
C50	4.10	5.94	7.13	3.66	1.94
C75	3.24	5.97	7.19	3.81	1.82
C100	2.40	6.00	7.20	3.91	1.75
B0	2.02	6.06	4.04	2.14	1.30
B25	2.86	5.72	4.57	2.26	1.22
B50	3.63	5.42	5.07	2.26	1.38
B75	4.30	5.15	5.50	2.33	1.43
B100	4.91	4.91	5.89	2.42	1.38

cohesive energy density (see below) would display the same trends as in Fig. 4. These results call for two comments.

(1) The crosslink density n and the glass transition temperature T_g have little or no influence on rigidity in the glassy state. It is noteworthy that the highest E_T value corresponds to the lowest T_g value (C100).

(2) Globally, the modulus increases with the hydroxyl concentration (Fig. 4) which suggests that hydrogen bonding plays an important role in the elastic behaviour of these materials. The very strong effect of aniline (series C) remains, however, unexplained since the overall composition of these systems is very close to the TGAP-DDM (A100) composition and their packing density ρ^* is slightly lower (Table I).

3.2. Dynamic moduli (0.3 Hz)

Some typical modulus-temperature curves are presented in Fig. 5. They display generally two secondary transitions: T_β near 210 to 250 K and T_β' near 320 to 340 K. The nature of the corresponding relaxations

will not be discussed here. The modulus values E_D' at 293 K are given in Table II. There are two comments on these results.

(1) Despite a considerable scatter, it may be observed that the hierarchy of dynamic moduli is globally the same as the one of static tensile moduli measured at the same temperature.

(2) The precedingly found "abnormal" behaviour of sample C (aniline) disappears at $T < T_\beta$ (Fig. 5). These results could be consistent with the hypothesis that aniline suppresses at least partially the β relaxation, which could explain the decrease of the modulus gap at T_β and the higher rigidity of aniline systems at $T > T_\beta$.

3.3. Ultrasonic moduli (5 MHz)

The propagation velocities of longitudinal (v_L) and transversal (v_T) waves measured at 20°C are listed in Table III with the corresponding moduli and Poisson's ratios. The values of these latter (0.36–0.38) are in good agreement with the previously reported data [9].

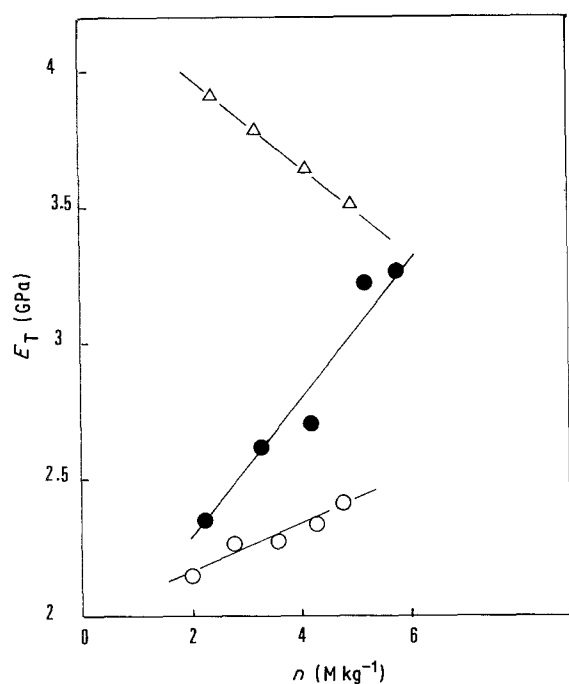


Figure 3 Tensile modulus versus crosslink density (●) series A, (○) series B, (△) series C.

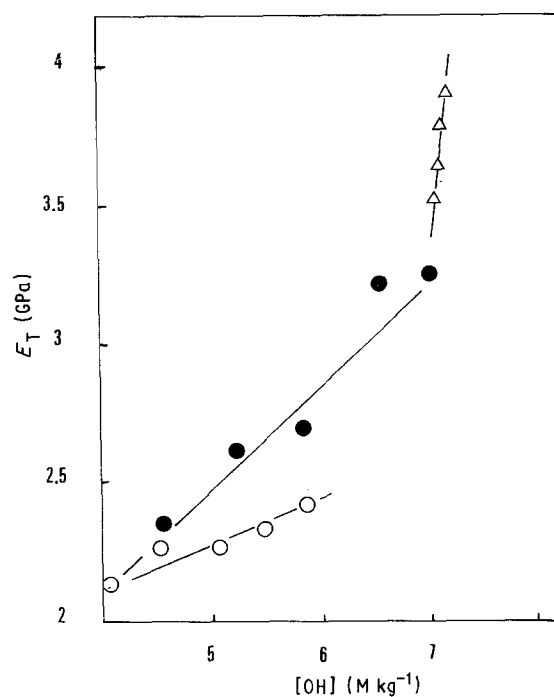


Figure 4 Tensile modulus versus hydroxyl concentration. Same symbols as in Fig. 3.

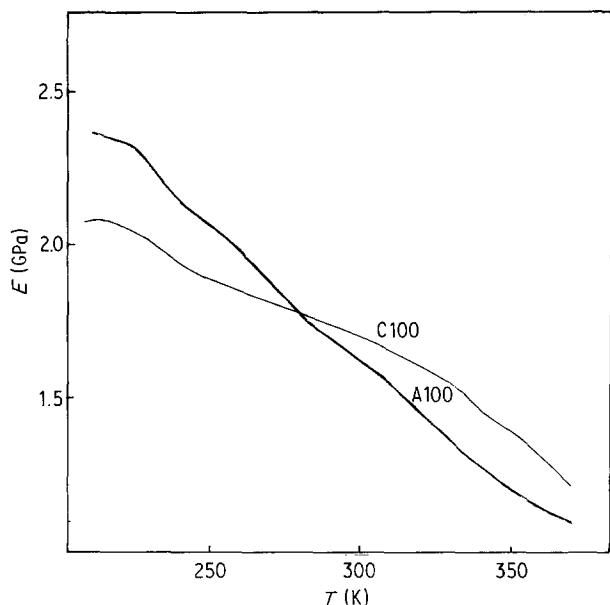


Figure 5 Dynamic modulus versus temperature (in the glassy state) for some samples under study.

They decrease slightly with the rigidity. In series A and B, the hierarchy of modulus values is the same as precedingly found. In contrast, aniline systems are less rigid than their parent system TGAP-DDM (A100). This seems to be a confirmation of the previous hypothesis on the suppression of the beta relaxation by aniline since it is reasonable to assume that, as a consequence of the thermally activated character of beta motions, T_β must be higher than the room temperature at 5 MHz frequency as shown by dielectric measurements on similar systems [10].

4. Discussion

4.1. Molecular structure dependence

When the influence of beta relaxations is negligible e.g. in the case of ultrasonic measurements in this study, the modulus is only dependent on the molecular structure and reflects essentially the intensity of cohesive forces. We found it interesting to compare three approaches of the structure-modulus relationship which gave relatively good results in the case of linear polymers [11]. In all cases, a network “monomer

unit”, as defined in the preceding parts of this article, was used for the calculations. Its molar mass.

4.1.1. Rao's approach [8, 11, 12]

It is assumed that

$$v_L = \left(\frac{U}{V}\right)^6 \left(\frac{3(1-\nu)}{(1+\nu)}\right)^{1/2} \quad (4)$$

where U is the sum of the molar contributions U_1 of all the groups of the “monomer unit”. Using the U_1 values recommended by Van Krevelen and Hoftyzer [11], v_L was calculated for all the samples under study. The results (Table III), show a systematic underestimation, although a satisfactory order of magnitude was obtained. It seems that the contribution of hydroxyl groups, (e.g. of hydrogen bonding) is underestimated.

4.1.2. Bondi's approach

Bondi [13] proposed for $T < 0.9 T_g$

$$E = \frac{H_s}{V_w} \left[E_0^* \left(1 - \frac{30}{E_0^{*2}} \frac{T}{T_g} \right) \right] \quad (5)$$

where $E_0^* = 85.9 \rho^* - 47.6$.

The values of H_s/V_w (see Appendix) are ranged between 0.87 and 1.04 GPa. They are generally higher than those of moderately polar linear polymers, but lower than those of very polar aromatic polyamides or polyimides ($H_s/V_w = 1.1$ to 1.4 GPa). The reduced modulus E_0^* is about 10 to 13 for the systems under study, so that $E \approx 10 H_s/V_w$. Thus, the modulus is noticeably overestimated by this prediction method.

4.1.3. Grüneisen's approach

For molecular crystals, Grüneisen [14, 15] proposed $B = 8.04 H_s/V$ which was transformed into $B = 8.04 E_{coh}/V$ for amorphous polymers [11]. The molar group contributions to sublimation energy H_s and cohesive energy E_{coh} must be, by definition, the same. However significant discrepancies can be observed from one author to another as shown in the Appendix. In Fig. 6, B_u was plotted against cohesive energy density according to Fedor's [16]. A relatively good linear correlation can be observed, but the

TABLE III Propagation rate of ultrasonic waves, moduli and Poisson's ratio, cohesive energy density parameters and water equilibrium concentration at 100°C, 95% RH

Code	V_L (e) (m sec ⁻¹)	V_L (calc) (a) (m sec ⁻¹)	V_T (m sec ⁻¹)	E_u (GPa)	B_u (GPa)	G_u (GPa)	ν	E_{coh}/V (GPa)	H_s/V_w (GPa)	w_m (%)
A0	2691	2317	1219	4.89	6.31	1.78	0.371	0.553	0.88	2.54
A25	2763	2353	1253	5.24	6.75	1.90	0.371	0.580	0.92	3.40
A50	2831	2445	1287	5.61	7.18	2.05	0.370	0.609	0.95	4.36
A80	2910	2504	1320	6.00	7.72	2.19	0.370	0.639	0.99	5.50
A100	2972	2604	1372	6.51	8.02	2.38	0.365	0.658	1.01	6.09
C25	2983	2314	1349	6.30	8.17	2.29	0.372	0.656	1.02	5.47
C50	2953	2367	1326	6.10	8.05	2.22	0.374	0.658	1.02	4.98
C75	2905	2424	1337	6.14	7.62	2.25	0.366	0.656	1.03	4.92
B0	2541	2238	1134	4.07	5.46	1.48	0.376	0.511	0.88	1.81
B25	2586	2302	1162	4.28	5.64	1.56	0.374	0.528	0.90	2.26
B50	2626	2645	1185	4.48	5.84	1.63	0.372	0.542	0.93	2.68
B75	2683	2300	1214	4.74	6.13	1.73	0.371	0.558	0.95	3.08
B100	2696	2525	1223	4.86	6.67	1.77	0.368	0.569	0.97	3.52

(a) longitudinal velocity calculated from the Rao function (see the text).

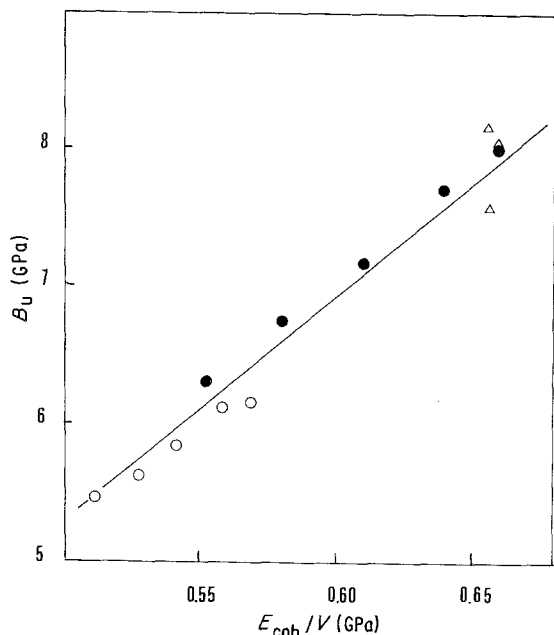


Figure 6 Ultrasonic bulk modulus versus cohesive energy density. Same symbols as in Fig. 3.

proportionality constant is significantly higher than the previously reported one: 11.5 ± 1 against 8.04.

4.1.4. Hydrogen bonding approach

It was found, many years ago, that hydrogen bonding increases the sound velocity in molecular liquids and that intramolecular bonds have a low influence compared to intermolecular ones, which was interpreted in terms of intermolecular spacing [17]. A recent study showed that, in amine crosslinked epoxies, intermolecular (OH-OH) and intramolecular (OH-N) bonds coexist in concentration ratios depending strongly on the amine nucleophilicity among others structural factors [18]. Thus, whatever the physical meaning of a given additive law for a modulus prediction, it must be reasonably presumed that the hydrogen bonding component is especially high. The nature of hydrogen bonds must be taken into account, which is not the case in the preceding approaches based on the implicit hypothesis that the group molar contributions are not interdependent.

It is interesting to note that the water equilibrium concentration w_m , determined by a classical sorption experiment, can be more or less considered as a measure of the concentration of available intermolecularly bonded hydroxyls. The higher is the amine nucleophilicity, or eventually steric hindrance, the higher is the concentration of intramolecular bonds (OH-N) and the lower is the water solubility [19].

In Fig. 7, the ultrasonic moduli were plotted against equilibrium water concentration w_m determined at 100°C, 95% r.h. (see the preceding part of this article). A practically linear correlation can be observed. In the series A and B, the modulus increases with the hydroxyl concentration. In the series C, where this concentration is almost constant, the modulus decreases slightly with the aniline fraction because (OH-N) bonding is more favoured in aniline systems than in DDM ones as shown by IR spectrophotometry [18]. The correlation between modulus and water solubility

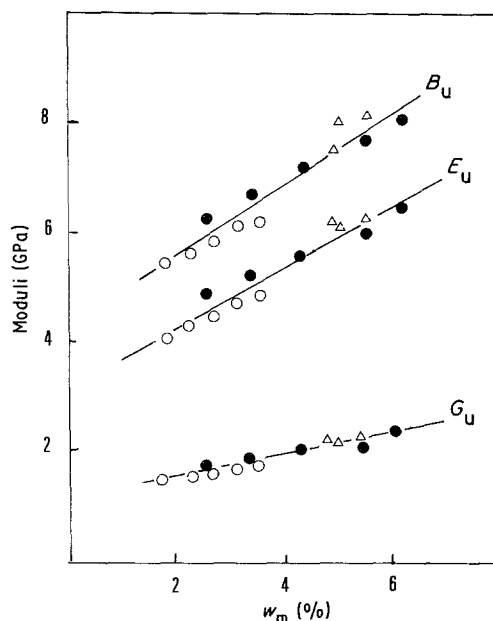


Figure 7 Ultrasonic moduli (of dry samples) against water equilibrium concentration measured at 100°C, 95°C r.h. (●) series A, (○) series B, (△) series C.

seems therefore not to be a coincidence. The relation is expressed by the following equation

$$M = M_0 + kw_m \quad (6)$$

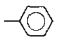
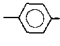
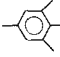
where M is the modulus. The slope k would express essentially the contribution of hydrogen bonding interactions and the intercept M_0 would be linked to the contribution of non-hydrophilic groups, mainly hydrocarbon ones, via dispersion forces. M_0 would presumably vary with the aromatic group concentration since $B_0 \approx 2$ GPa for linear aliphatic hydrocarbon polymers, ≈ 5 GPa for polystyrene [11] and ≈ 4.5 GPa for the systems under study. The small variations in the concentration of aromatic nuclei in the series under study (4.9 to 6.8 M kg⁻¹) do not allow their influence to be quantified.

4.2. Viscoelastic effects

In conditions where viscoelastic effects become noticeable, e.g. for room temperature tensile testing at moderate strain rate, the elasticity remains governed by cohesion or hydrogen bonding, see for instance Fig. 4. However, other physical variables are also to be taken into account. In many cases, a plasticization, e.g. a T_g decrease, coincides with rigidity increase in the glassy state. This was observed as well for non-stoichiometric systems [1-3], as when a reactive diluent was used [20]. This could be a very general phenomenon since plasticized polyvinylchloride [21] or polycarbonate [22] display the same behaviour. In all predicted cases, it was found that the density increases with the extent of plasticization, which was interpreted in terms of packing density increase or decrease of the free volume fraction. However, this is not the case for the aniline systems under study: although they display clearly the previously described features, their density ρ and packing density ρ^* decrease with the aniline concentration (Table I), whereas their modulus increases.

In the case of linear polymers [21, 22] and epoxy-reactive diluent [20] systems, the authors observed, as

TABLE IV Molar contributions to the sublimation enthalpy, cohesive energy, 'Van der Waals' volume and Rao's function, used for the calculations

Structural Unit	H_s (kJ mol ⁻¹)	E_{coh} (kJ mol ⁻¹)	V_w (cm ³ mol ⁻¹)	U (cm ^{10/3} s ^{-1/3} mol ⁻¹)
-CH ₂ -	8.36	4.04	10.23	800
-CH ₂ -CH ₃	17.89	8.75	23.90	2200
>C(CH ₃) ₂	12.12	10.89	30.67	2850
	35.11	31.94	45.84	4650
	29.26	31.94	43.32	4100
	28.42	31.94	38.28	3350
-O-	6.48	3.35	3.50	400
>CH-OH	34.28	29.80	14.82	1050
-N<	0	4.19	4.33	100

for aniline systems in this study, a partial or total disappearance of the dissipation band due to beta motions in the thermomechanical spectra ($\tan \delta$ or $E'' - T$). These latter were not examined by the authors who studied the non-stoichiometric epoxy systems [1-3], but in similar cases, Williams showed also that the side chains, having an unreacted epoxide group at their free extremity, are inactive in beta relaxations [23]. This seems therefore a common feature for all systems in which the plasticization increases the rigidity in the glassy state. Two hypotheses come to mind. According to the first, the beta transition would be shifted to lower temperature, out of the observation range, and according to the second, it would be suppressed. The fact that the plasticization increases the low frequency modulus at $T > T_\beta$ but does not influence in the same way the high frequency (ultrasonic) modulus, is obviously in favour of the second hypothesis, at least for the aniline systems. Since the hypothesis of a packing density increase can be rejected, the mechanism of the beta transition suppression remains unexplained and needs further investigations.

5. Conclusions

Two main conclusions can be derived from the above study.

(1) The elastic properties of epoxide-amine networks in the glassy state are mainly linked to the cohesive energy. The classical additive laws for their prediction cannot however be applied, owing to the great importance of hydrogen bonding which varies in a complex way with various structural factors, mainly the amine nucleophilicity. An interesting correlation was found between the moduli and the water equilibrium concentration which is essentially linked to the concentration of intermolecularly bonded hydroxyls.

(2) At $T > T_\beta$ and low strain rates, the beta relaxation decreases the moduli, but the ratio of network segments involved in beta motions decreases (the modulus increases) with the monoamine (aniline) content. This latter observation seems to be generalized to a wide variety of internal or external plasticizations.

Acknowledgement

This work was sponsored by "la Direction des

Recherches et Etudes Techniques" which is gratefully acknowledged.

Appendix

The packing density ρ^* is given by

$$\rho^* = v_w/V = \rho V_w/M \quad (\text{A1})$$

where $V_w = \Sigma V_{wi}$ is the 'Van der Waals' volume obtained by summation of the molar group contributions listed by Bondi [13]. The contribution of the tetrasubstituted aromatic unit was extrapolated from those of mono and disubstituted units.

H_s/V_w is the cohesive energy density parameter used by Bondi [13].

$H_s = \Sigma H_{si}$ is the sublimation enthalpy of a monomer unit.

E_{coh}/V is the cohesive energy density. It was hypothesized that $E_{\text{coh}} = \Sigma E_{\text{cohi}}$. In principle, $E_{\text{coh}} = H_s$. We used two series of data from two distinct sources [13, 16], in order to illustrate the possible discrepancies in this field.

$U = \Sigma U_i$ is the Rao's function group contribution.

All the elemental group contributions used for the calculations are listed in Table IV.

References

1. W. N. FINDLEY and R. M. REED, *Polym. Eng. Sci.* **27** (1977) 837.
2. R. J. MORGAN, *Adv. Polym. Sci.* **72** (1985) 1.
3. V. B. GUPTA, L. T. DRZAL, C. Y. C. LEE and M. J. RICH, *Polym. Eng. Sci.* **25** (1985) 812.
4. S. C. MISRA, J. A. MANSON and L. H. SPERLING, *American Chemical Society Symp. Ser.* **114** (1979) 137.
5. P. C. BABAYEVSKY and J. K. GILHAM, *J. Appl. Polym. Sci.* **17** (1973) 2067.
6. M. CIZMECIOGLU, A. GUPTA and R. F. FEDORS, *J. Appl. Polym. Sci.* **32** (1986) 6177.
7. R. A. KLINE and D. M. EGGLE, *Non Destructive Testing International* **19** (1986) 341.
8. J. SCHUYER, *J. Polym. Sci.* **36** (1959) 475.
9. P. S. THEOCARIS and C. HADJIJOSEPH, *Kolloid. Z.* **202** (1965) 133.
10. See for instance J. D. Reid, W. L. Lawrence and R. F. Buck, *J. Appl. Polym. Sci.* **31** (1986) 1771.
11. D. W. VAN KREVELEN and P. J. HOFTYZER, in "Properties of polymers, their estimation and correlation with chemical structure" 2nd Edn. (Elsevier, Amsterdam, 1976) Ch. 3.
12. R. RAO, *J. Chem. Phys.* **9**, (1941), 682.

13. A. BONDI, in "Physical properties of molecular crystals, liquids and glasses" (Wiley, New York,, 1968) pp. 390-394, 444.
14. E. GRÜNEISEN ed., "Handbuch der Physik", Vol. 10 (Springer, Berlin, 1926) p. 52.
15. A. V. TOBOLSKI ed., "Properties and structure of polymers", (Wiley, New York, 1960).
16. R. F. FEDORS, *Polym. Eng. Sci.* **14** (1974) 147.
17. G. C. PIMENTEL and A. L. McCLELLAN, in "The Hydrogen Bond", Ch. 2 (W. H. Freeman Co, San Francisco, 1960) p. 58.
18. V. BELLENGER, J. FRANCILLETTE, P. HOAREAU, E. MOREL and J. VERDU, *Polymer* **28** (1987) 1079.
19. V. BELLENGER, E. MOREL and J. VERDU, *Polymer* **26** (1985) 1719.
20. J. DALY, A. BRITTEN, A. GARTON and P. D. McLEAN, *J. Appl. Polym. Sci.* **29** (1984) 1403.
21. L. BOHN, *Kunststoffe* **53** (1963) 826.
22. L. M. ROBESON and J. A. FAUCHER, *J. Polym. Sci.* **B7**, (1969) 35.
23. J. G. WILLIAMS, *J. Appl. Polym. Sci.* **23** (1979) 3433.

*Received 23 November 1987
and accepted 29 April 1988*